

ORIGINAL RESEARCH ARTICLE

# Impacts of land use and land cover changes on groundwater recharge in the Dire Dawa watershed, Ethiopia

Tariku Takele<sup>1\*</sup>, Adula Bayisa<sup>2</sup>, and Muralitharan Jothimani<sup>3</sup>

<sup>1</sup>Department of Geology, College of Natural and Computational Sciences, Dilla University, P.O. Box 419, Dilla, Ethiopia

<sup>2</sup>Groundwater resource study and Design, Ministry of Water and Energy, P.O.Box-5744, Addis Ababa, Ethiopia

<sup>3</sup>Department of Geology, College of Natural and Computational Sciences, Arba Minch University, P.O. Box 21, Arba Minch, Ethiopia

\*Corresponding author: Tariku Takele (tariku.takele@du.edu.et)

*Received: May 4, 2025; 1st revised: June 13, 2025; 2nd revised: June 22, 2025; Accepted: June 25, 2025;  
Published online: August 22, 2025*

**Abstract:** Land use and land cover (LULC) change is a growing global concern, particularly in water-scarce regions, where it directly influences hydrological systems and groundwater sustainability. The Dire Dawa watershed in eastern Ethiopia exemplifies this challenge. This study investigates the impacts of LULC changes on groundwater recharge in the Dire Dawa watershed from 2000 to 2022. The LULC changes were analyzed using ERDAS IMAGINE 2015 and geographic information systems, while the effects on groundwater recharge were assessed using the Soil and Water Assessment Tool (SWAT) model. The performance of the SWAT model was evaluated using the sequential uncertainty fitting 2 technique, demonstrating good model performance, with  $R^2$  values of 0.84 (calibration) and 0.79 (validation), Nash-Sutcliffe efficiency values of 0.75 and 0.72, and percent bias values of -0.1 and -11, respectively. The results indicated that, over the 22 years, agricultural land expanded by 52.6%, while built-up areas increased by nearly 79.2%. In contrast, shrublands and forests declined by 23.7% and 62.8%, respectively. These shifts resulted in a 24.5% reduction in groundwater recharge (-48.8 mm/y) and a 19.9% increase in surface runoff (42.8 mm/y). These findings reflect broader regional patterns and emphasize the importance of integrated land and water resource management to support ecological stability and community resilience.

**Keywords:** Dire Dawa watershed; Land use and land cover change; Groundwater recharge; Soil and water assessment tool; Image processing

## 1. Introduction

Groundwater is one of the most essential yet often overlooked natural resources that sustain life on Earth. It serves as a critical backbone for ecosystems, agriculture, and the daily needs of billions of people worldwide. In regions where surface water is limited or unpredictable, groundwater becomes the primary, sometimes the only

source of water security.<sup>1</sup> This resource is integral to ensuring water security, particularly as urbanization, industrialization, and climate change continue to reshape our environment.<sup>2-5</sup> As the pressures of rapid urbanization, industrial growth, and climate change intensify, safeguarding groundwater is no longer a local challenge; it is a global imperative. Recognizing its value is not just about hydrology or resource management; it

is about securing a sustainable and dignified future for humanity and the planet we share.<sup>6,7</sup>

Land use and land cover (LULC) and climate change, in particular, are disrupting vital processes such as groundwater recharge, surface runoff, and overall watershed hydrology, making it even harder to manage and sustain these resources.<sup>8-10</sup> Furthermore, LULC changes, driven by both urban sprawl and industrial growth, have compounded these challenges, particularly in arid and semi-arid regions where water scarcity is already a pressing concern.<sup>11,12</sup>

Understanding how LULC changes affect groundwater recharge is vital, especially as urban areas expand and natural landscapes transform.<sup>4,13,14</sup> These changes disrupt the natural water balance, impacting ecosystems, agriculture, and the daily lives of communities. Groundwater sustainability, therefore, is not only a scientific challenge but also a pressing human concern.<sup>9</sup> Effective groundwater management is crucial for preserving ecosystem health and maintaining watershed functionality.<sup>15,16</sup> Without it, groundwater depletion could lead to severe consequences, including increased water scarcity and ecological degradation at both local and regional scales.<sup>17,18</sup>

In response to these challenges, the Soil and Water Assessment Tool (SWAT) has emerged as an essential tool in groundwater studies.<sup>14,19,20</sup> When combined with geographical information systems (GIS) and remote sensing data, SWAT provides a robust and integrated framework for evaluating the influence of environmental factors on water balance components across various watershed scales.<sup>21,22</sup> Its ability to simulate spatial and temporal variations makes the SWAT particularly effective in regions facing environmental stressors, such as climate change and rapid urbanization.<sup>4,9,23</sup> This modeling capacity is especially relevant in vulnerable areas, such as the Dire Dawa watershed in eastern Ethiopia, where shifting LULC patterns and climate variability necessitate informed, scenario-based analyses to support sustainable water management.

In Ethiopia, groundwater is a critical resource for irrigation, industrial use, and domestic consumption. However, the country's water resources are under increasing stress due to rapid urbanization, population growth, and climate variability.<sup>3,24,25</sup> Accurate assessments of groundwater recharge potential are essential for guiding sustainable water management practices and ensuring long-term water security.<sup>3,26</sup> The Dire Dawa watershed in Ethiopia's Awash River basin (Figure 1) exemplifies these challenges. As urbanization and industrial activities have grown,

local water resources have been depleted for several decades.<sup>27-29</sup> Despite growing concerns over water scarcity, groundwater depletion and the LULC changes in the region have impacted the groundwater potential of the area.

This study aims to investigate the impacts of LULC changes on groundwater recharge in the Dire Dawa watershed in Ethiopia from 2000 to 2022. Unlike previous research that primarily focused on surface runoff and flood hazards<sup>30</sup> or employed broader spatial models, such as WetSpa, to estimate groundwater recharge,<sup>31</sup> a process-based and temporally detailed simulation was utilized in this study using the SWAT. By integrating recent LULC data with hydrological modeling, a more comprehensive understanding of how landscape changes influence groundwater availability is provided, addressing a gap that has not yet been fully explored in the Dire Dawa context.

The analysis of this study's results offers insights into sustainable watershed management. It contributes to Ethiopia's broader climate resilience efforts, including the Green Legacy Initiative, which serves as an essential component of national environmental policies, focusing on reforestation and conservation goals.<sup>32</sup> The efforts made toward reforestation directly contribute to groundwater recharge through their impact on the infiltration of soil water, reduction of surface runoff, and improvement of groundwater recharge dynamics. The sustainability and long-term water security of the local water resources in the region depend on these conservation methods, which aim to mitigate environmental degradation and promote sustainable resource management.<sup>32</sup>

## 2. Methodology

### 2.1. Study area

#### 2.1.1. Geographical setting

The Dire Dawa watershed is situated in eastern Ethiopia, within the Awash River basin, south of the Afar Depression. It is located between latitudes 9°26'00" and 9°45'30" N and longitudes 41°41'00"–42°06'30" E, approximately 515 km from Addis Ababa (Figure 1).

The research area is situated within a semi-arid zone, and the match between climate and landform is a crucial factor in determining water resources. Located in the basin of the foothills surrounding the mountains, the catchment is supplied by several rivers, the largest of which cuts through the area's core. The region experiences a bimodal rainfall pattern, with the highest rainfall intensities occurring between July and

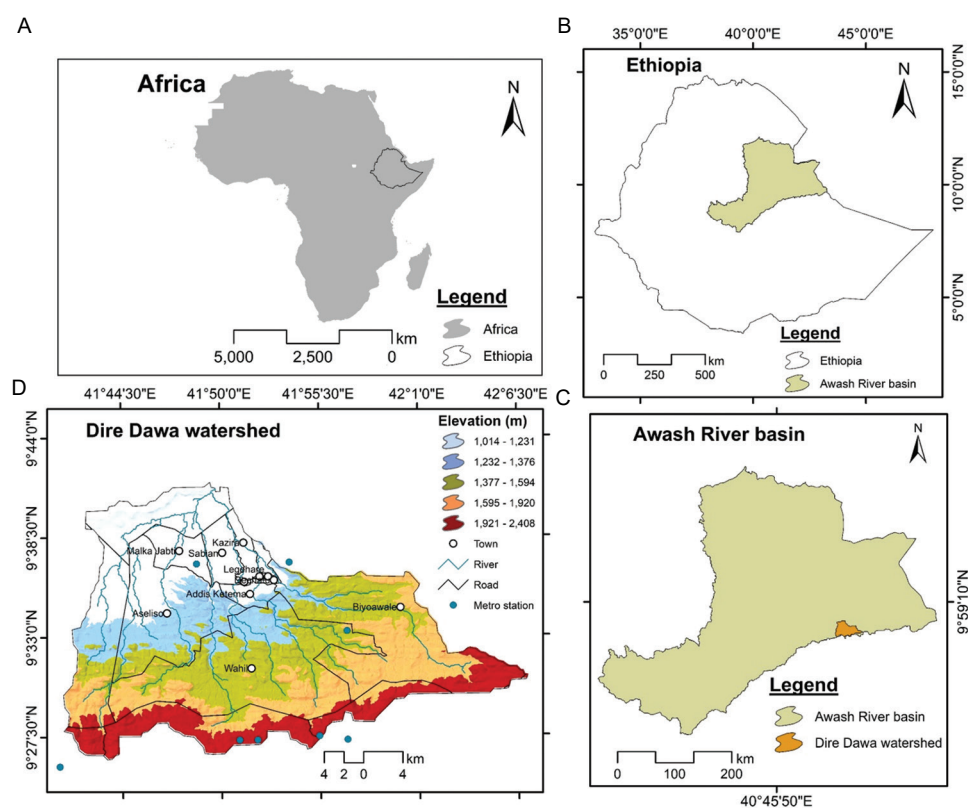


**Figure 1.** Maps depicting the location of the study area: (A) Ethiopia; (B) Awash river basin; and (C) the study site (Dire Dawa watershed). Maps acquired from <https://www.ethiopia-maps.org/>; <https://search.earthdata.nasa.gov/>

September, reaching up to 450 mm. The dry season spans from November to February, resulting in strong seasonal differences in water resources. The weather is usually mild (9.8–20.9°C), and the two warmest months are February and March. Under this climate, the cyclic changes in rainfall play a crucial role in shaping the runoff and groundwater recharge patterns. During the rainy season, the land experiences high runoff, resulting in water scarcity. The landscape is characterized by a diverse mix of plateaus, escarpments, and valleys, all of which are shaped by volcanic activity. With elevations ranging from 1,014 m to 2,408 m, the area encompasses steep mountains, flat plains, and fault-induced landforms, including half-grabens and horsts. These landforms directly impact how water moves through the region. The steep slopes and rocky surfaces result in high runoff and limited water retention, particularly during intense rainfall.

### 2.1.2. Geological and hydrogeological setting

The geology of the Dire Dawa region is characterized by ancient Precambrian basement rocks overlain by Mesozoic sedimentary formations, including the

Adigrat sandstone, Hamaneli limestone, and Amba Aradam sandstone. These units, together with the Tertiary volcanic basalts from the Afar volcanic series and the recent Quaternary alluvial deposits, form the main hydrogeological framework. The Precambrian basement rocks are highly weathered and fractured, creating secondary porosity; however, the porous sandstones and limestones serve as the region's primary aquifers. The volcanic basalts contribute to groundwater flow predominantly through fractures and weathered zones. The Quaternary alluvial sediments, particularly in the lower-elevation areas within the Afar Depression, are significant groundwater reservoirs.

The groundwater flow in the area is strongly influenced by major fault systems associated with the East African Rift and the Afar Depression tectonics, creating zones of enhanced permeability and acting as preferential flow pathways. The hydrogeology of the Dire Dawa watershed is shaped by the complex interaction of geological formations, tectonic activity, and the region's varied topography. Groundwater occurs mainly in two primary systems: the rugged escarpment and the adjacent plains. The escarpment features a complex geology composed

of sedimentary, basement, and volcanic rocks, and is deeply fractured by predominantly east-west trending faults, significantly influencing groundwater flow and availability (Figure 2).

In contrast, the basin at the foot of the escarpment is dominated by thick alluvial deposits, forming extensive aquifers that serve as crucial water sources for local communities. These alluvial aquifers display variable thicknesses and sediment types, resulting in fluctuating groundwater levels and transmissivity rates. Volcanic rock formations in the elevated areas generally yield limited groundwater, except in localized zones. Meanwhile, the upper sandstone layers exhibit moderate to high groundwater potential, reflecting their variable permeability and porosity.

**2.2. Datasets and methods**

Figure 3 presents the methodology applied in this study

**2.2.1. Datasets**

This study employed a modeling approach to assess the impact of land-use changes on groundwater recharge, integrating various datasets (Table 1). Meteorological data were sourced from the Ethiopian Meteorological Institute’s river flow data from the Ministry of Water and

Energy, and spatial data from remote sensing, GIS, and global positioning systems (GPS). These datasets were used to develop a conceptual framework illustrating how land cover alterations influence groundwater systems. Meteorological data were collected from eight stations within the watershed, supplemented by the data from the

**Table 1. Data sources and details**

Data type (resolution)	Data source/references
Digital elevation model (12.5 m×12.5 m)	Earthdata Search ( <a href="https://search.earthdata.nasa.gov/">https://search.earthdata.nasa.gov/</a> )
Landsat images (30 m×30 m)	USGS ( <a href="https://earthexplorer.usgs.gov/">https://earthexplorer.usgs.gov/</a> )
Precipitation and temperature (daily)	Ethiopian Meteorological Institute ( <a href="https://www.ethiomet.gov.et/">https://www.ethiomet.gov.et/</a> )
Geological map (shape file)	Mapserver Ethiopia: <a href="https://www.ethiogis-mapserver.org/">https://www.ethiogis-mapserver.org/</a>
Daily discharge (daily)	Ministry of Water and Energy of Ethiopia
Soil data (12.5 m×12.5 m)	FAO ( <a href="https://www.fao.org/ethiopia/en/">https://www.fao.org/ethiopia/en/</a> )

Abbreviations: FAO: Food and agriculture organization; USGS: United States geological survey.

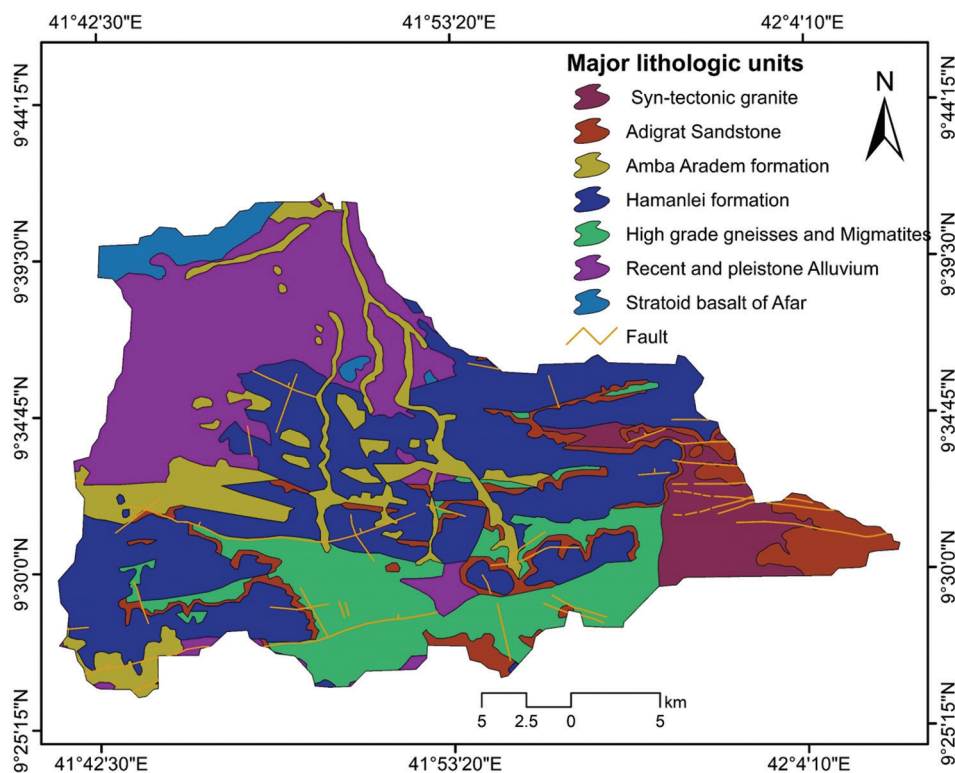


**Figure 2. Simplified geological map of the study area. Map acquired from: <https://www.ethiogis-mapserver.org/>**

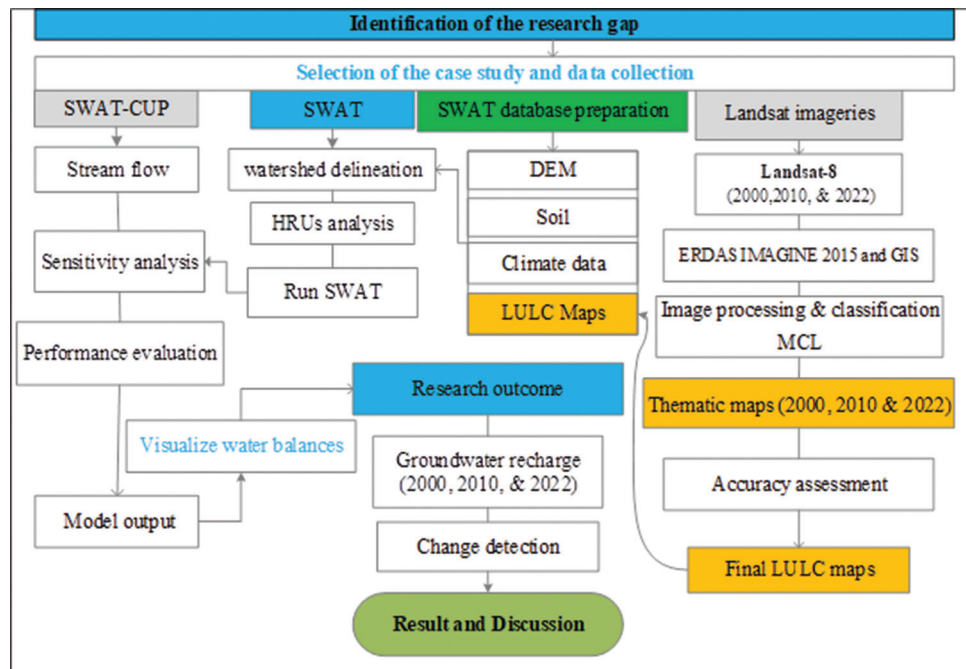


**Figure 3. Methodologies in this study**

Abbreviations: CUP: Calibration and uncertainty program; DEM: Digital elevation model; GIS: Geographical information system; HRU: Hydrological response units; LULC: Land use and land cover; MLC: Maximum likelihood classification; SWAT: Soil and water assessment tool.

nearest station with a long-term, continuous record. The dataset spans the period from 1979 to 2022 and includes variables such as evapotranspiration, temperature, relative humidity, sunshine hours, and wind speed. Due to the presence of missing or inconsistent data, an averaging method was applied for bias correction. Stations with significant data gaps were excluded from the analysis.

### 2.2.2. LULC analysis

The LULC detection and change analysis for the target watershed were performed with ERDAS IMAGINE 2015 (Hexagon, Sweden) and ArcGIS 10.8 software (Esri, United States). In this study, satellite images with cloud cover <10% of the imagery were selected to acquire accurate LULC data (Table 2). Landsat 7 was used for the 2000 LULC map, Landsat 5 for the 2010 LULC map, and Landsat 8 for the 2022 LULC map. Image processing and classifications were conducted using algorithms such as contrast enhancement, edge detection, and haze correction to enhance the satellite images based on the ERDAS IMAGINE 2015 software. The maximum likelihood classification method was employed, based on region-specific training information, to delineate LULC within the watershed. This algorithm has been used previously.<sup>33</sup>

### 2.2.3. Accuracy assessment of LULC map

The accuracy of remote sensing classifications is crucial to ensure that the classifications are consistent with field-grade reference data.<sup>3,34,35</sup> The classification of LULC types was further validated by the researchers' experiences, literature reviews, and Google Earth Pro. This study utilized both qualitative and quantitative methodologies, adhering to established scientific recommendations.<sup>35</sup> One of the most popular tools for achieving this is the confusion matrix, from which important measures such as overall accuracy (OA), producer's accuracy (PA), user accuracy (UA), and the kappa coefficient ( $\kappa_c$ ) can be derived. OA is a measure of global classification accuracy, while UA is a measure of the ability of a pixel classified in the presumed category to be similar to the real-world category. PA represents the proportion of a map in which a reference pixel is correctly classified, whereas  $\kappa_c$  represents the proportion of agreement between the classification and reference data after correcting for chance. The  $\kappa_c$  values have the following interpretations: >0.80 indicates high agreement, 0.40–0.80 indicates moderate agreement, and <0.40 indicates poor agreement<sup>35,36</sup> The  $\kappa_c$  was calculated using Equation I:

$$\kappa_c = \frac{\sum_i (N_{ii} - x)}{N^2 - x} \quad (I)$$

**Table 2. Satellite imagery used for watershed analysis**

Satellite/sensor	Resolution	Path/row	Acquisition date	Cloud cover (%)
Landsat 7	30 m×30 m	166/053	January 22, 2000	<10
Landsat 5	30 m×30 m	166/053	January 25, 2010	<10
Landsat 8	30 m×30 m	166/053	January 26, 2022	<10

where  $N$  is the total number of observations (the sum of all pixels in the confusion matrix),  $N_{ii}$  represents the correct classifications (values along the matrix diagonal), and  $x$  accounts for the expected agreement due to chance, based on the row and column totals of the matrix. This approach offers a comprehensive classification accuracy assessment, considering both actual data and potential random misclassification. Accuracy was validated using Google Earth imagery and field data, with metrics such as UA, PA, and  $\kappa_c$ . The final reclassification ensured a reliable depiction of land-use changes, supporting informed land management decisions for environmental sustainability.

#### 2.2.4. LULC change detection

This study employed a post-classification image comparison method to analyze LULC changes over 3 time periods: 2000–2010, 2010–2022, and 2000–2022. Satellite images for each reference year were classified independently and compared to assess shifts in land cover. LULC changes over the past two decades were evaluated in three 10-year intervals, starting from 2000. To calculate the relative percentage of change (P), the area of each land cover type at the start and end of each period was compared (Equation II):

$$P(\%) = \frac{(A_{L_f} - A_{L_i})}{A_{L_i}} \times 100 \quad (\text{II})$$

where  $A_{L_f}$  is the area at the final time point (2010 or 2022) and  $A_{L_i}$  is the area at the initial time point (2000 or 2010). In addition, the rate of change ( $\Delta R$ ) was calculated to assess the speed of land cover transitions (Equation III):

$$\Delta R = \left( \frac{A_{L_f} - A_{L_i}}{T} \right) \quad (\text{III})$$

where  $T$  is the number of years in the period. These calculations provide insight into how land use has evolved, offering valuable information on its effects on local resources and ecosystems, and informing sustainable land management strategies.

#### 2.2.5. The SWAT model development and input datasets

The SWAT model has been widely applied for hydrological modeling due to its user-friendly interface and convenient access to datasets for hydrological analysis. Alongside SWAT, the SWAT calibration and uncertainty program (SWAT-CUP) is commonly used to evaluate the performance of the SWAT model.<sup>37</sup> SWAT-CUP helps with calibrating and validating SWAT models, and it integrates several advanced algorithms, such as sequential uncertainty fitting (SUFI-2), generalized likelihood uncertainty estimation, parameter solution, Markov chain Monte Carlo, and particle swarm optimization.<sup>37,38</sup> These algorithms are used for sensitivity analysis, uncertainty analysis, and performance analysis. Various objective functions, including the coefficient of determination ( $R^2$ ), Nash-Sutcliffe efficiency (NSE), and percent bias (PBIAS), improve the model accuracy and reliability. Among these algorithms, SUFI-2 was chosen in this study as it has been widely used in hydrological modeling and is known for its ability to quantify model uncertainty and optimize calibration effectively.<sup>8,20</sup>

#### 2.2.6. SWAT input datasets

##### 2.2.6.1. Digital elevation model (DEM)

This study obtained a free 12.5 m × 12.5 m spatial resolution DEM from the Earthdata Search database (Table 1). The database is one of the key data sources for various applications, including watershed delineation, slope, and drainage network and pattern calculations, all of which are used to simulate water balance using SWAT modeling. The DEM was pre-processed in ArcGIS 10.8, where null values were filled using the spatial analysis tools in ArcToolbox, and then incorporated into ArcSWAT for watershed delineation and parameterization following SWAT procedures. This approach ensures that the DEM is complete and ready for accurate analysis, effectively defining watershed boundaries and flow patterns. The hydrological features, such as watersheds, stream networks, and slopes, were derived from the region's DEM using the ArcSWAT model.

### 2.2.6.2. Slope map

The slope map was constructed from DEM-derived elevation data. The study area was discretized into five slope classes, each interpreted as having different levels of steepness. These classes were then further re-classified into percentages, providing a more readily recognizable picture of the five slope classes. They were created using ArcSWAT dunging model parametrizations based on slope percentage gradients of the study area. This was done to provide a more detailed description of the topography of the target region.

### 2.2.6.3. Soil data

In the Dire Dawa watershed, key soil characteristics, such as texture, bulk density, saturated hydraulic conductivity, and available water content, were re-established and input into the SWAT model for hydrological simulation. These features influence the water flow, infiltration, and runoff processes. Such soil information was manually entered into the file (soil.dat) using ArcSWAT to meet specific modeling needs. In addition, the calibration of soil parameters was at the core of improving the accuracy of water balance and runoff forecasts, considering local land-use management variables. This approach laid the groundwork for assessing recharge and land-use-associated effects at the watershed scale.

### 2.2.6.4. LULC

Land use has a significant impact on a watershed's hydrology. The LULC is a key variable determining groundwater recharge in a watershed. To validate the scenarios considered by the SWAT model, a realistic land-use map was generated to delineate the hydrological response units (HRUs). All six LULC types were assigned different codes for model feasibility and were associated with a SWAT code to assess the influence of different land covers on groundwater recharge during the study period (2000–2022).

### 2.2.6.5. Meteorological data

Accurate weather data are essential for the SWAT model; hence, daily precipitation and temperature data (1982–2022) were used in the study. These data were primarily sourced from the local weather stations within and around the watershed. In cases where data gaps existed, linear regression and arithmetic methods were employed to interpolate missing values. To address the uneven distribution of weather stations, local data were supplemented with records from the National Centers for Environmental Prediction's Climate Forecast System Reanalysis. All meteorological data were processed into

formats compatible with the SWAT model, ensuring seamless integration and reliable model inputs.

### 2.2.6.6. Hydrological data (river flow)

To substantiate the SWAT model, data on river discharge from observed gauging stations in the watershed were used. The discharge data from 2000 to 2014, collected from the Ministry of Water and Energy of Ethiopia, were analyzed to calibrate and validate the SWAT model. These data were of particular importance, as they tested and calibrated the model, assessing the fidelity with which the model can reproduce river flow patterns in the watershed. Hydrogeologists have continuously applied this observed data for watershed hydrological modeling. In this study, based on the availability of the data, discharge data spanning from 2000 to 2014 were utilized to calibrate and validate the SWAT model.

### 2.2.7. The SWAT model setup

The SWAT model was executed at a 12.5 m DEM in the Earthdata Search database to delineate the watershed. With the SWAT model, flexible modeling of hydrological processes can be achieved using the computationally efficient Soil Conservation Service (SCS) Curve Number (CN) procedure<sup>39</sup> for surface runoff calculation. ArcSWAT was downloaded for free (<https://swat.tamu.edu/software/arcsbat/>) based on ArcGIS (version 10.8). In this study, potential evapotranspiration was estimated using the Hargreaves techniques,<sup>40</sup> selected based on the availability of climate data. The calibration and validation of the model were performed using SWAT-CUP and the SUFI-2 algorithm, both of which are also recognized for producing accurate results with minimal iterations.<sup>38</sup> Detailed model equations and units are presented in the SWAT documents.<sup>41</sup> SWAT simulates the water balance components daily (Equation IV):

$$SW_t = SW_0 + \sum_{i=1}^t (R_{day} - Q_{surf} - E_a - W_{seep} - Q_{gw}) \quad (IV)$$

where  $SW_t$  is the final soil water content (mm) at time  $t$ ,  $SW_0$  is the initial soil water content at a  $t$  of 0 (or  $i = 0$ ),  $R_{day}$  is the total precipitation for day  $i$  (mm),  $Q_{surf}$  is the surface runoff for day  $i$  (mm),  $E_a$  is the evapotranspiration for day  $i$  (mm),  $W_{seep}$  is the inflow to the vadose zone from the soil profile for day  $i$  (mm), and  $Q_{gw}$  is the return flow for day  $i$  (mm). This equation considers the contributing factors in soil water processes, including precipitation, runoff, evapotranspiration, seepage, and return flow, and is used to model hydrological processes in watershed applications. ArcSWAT partitions the watershed into sub-basins and HRUs according to

soil type, slope, and land cover. The HRUs were superimposed with soil and land cover data to model elementary hydrological processes such as runoff and infiltration. Weather data (air temperature and rainfall) were employed to tune model performance. Soil data from National Agricultural institute were cross-checked with the Food and Agriculture Organization soil map, and slope and elevation maps were produced from the DEM of the region.

2.2.7.1. Watershed delineation and hydrologic response units  
Flow accumulation and direction were developed using ArcSWAT with the region's DEM. These steps are crucial for characterizing the watershed. This study divided the watershed into 30 sub-watersheds, facilitating the detailed visualization of hydrological units for the simulation of groundwater recharge employed in the SWAT model. The land use, soil, and slope data were combined to define HRUs using thresholds of 20% for land use, 10% for soil, and 20% for slope-based slope distribution of the region. This unit is one of the advances made by SWAT in simulating water balances for watersheds. These HRUs were employed to simulate hydrological processes (e.g., surface runoff and groundwater recharge) in the SWAT model.

#### 2.2.7.2. Weather data integration

Daily data on precipitation and temperature from eight weather stations were processed for the ArcSWAT model. Meteorological variables (e.g., humidity, wind speed, and solar radiation) for which values were unavailable were estimated using the Weather Generator (WGEN-USER), with default values derived from the United States' climate data. This merging of weather data, combined with watershed and HRU delineations, enabled the simulation of groundwater recharge using the procedures provided in the ArcSWAT model.

#### 2.2.7.3. Sensitivity analysis, model calibration, and model validation

Sensitivity analysis was conducted to understand the contribution of model input to the outputs, to calibrate the model, and to reduce uncertainty.<sup>8,37</sup> This process was crucial to enhancing the model's accuracy. During the process, some essential parameters for adjustment were identified, thereby reducing time and improving the accuracy of predictions.<sup>37,38</sup> The SWAT-CUP with the SUFI-2 methodology identified 13 parameters that significantly affected streamflow simulations (Table 3). These parameters were calibrated to align with local conditions, improving the model reliability.<sup>17,42</sup>

Focusing on these critical parameters enhanced the model accuracy, ensuring alignment with observed data and improving its ability to simulate future hydrological responses to changes in land use and climate. Detailed descriptions of the parameters are available in the SWAT user manual for replication or further refinement.<sup>43,44</sup>

In this study, both manual and automated techniques were employed using observed river flow data for SWAT model calibration. The combination of these approaches was chosen to ensure greater accuracy and reliability, as manual techniques allow for expert judgment, while automated methods enhance efficiency and minimize human error.<sup>13</sup> To allow the model to stabilize, the first 2 years (2000 and 2001) were excluded as a warm-up period, following established hydrological modeling practices.<sup>41</sup> Calibration was based on 2002–2007 data, while validation used 2008–2014 data. For manual calibration, parameters were adjusted through trial and error to enhance the model performance.<sup>38,43</sup> In addition, the SUFI-2 method was employed to fine-tune parameters within defined ranges, thereby improving accuracy through a robust statistical approach.<sup>17,45</sup> To evaluate the model performance, metrics such as  $R^2$ , NSE, and PBIAS were applied. Calibration was accepted as successful if the mean flow difference was within  $\pm 15\%$ ,  $R^2 > 0.60$ , and  $NSE > 0.50$ , as previously reported.<sup>8,45</sup> The results showed a strong correlation between the simulated and observed river discharge during validation, confirming the model's reliability for predicting future hydrological changes and responses to land-use changes and climate variations (Figure 4).

#### 2.2.7.4. Model performance metrics

Model validation demonstrated that a site-specific model could be used to predict without error, and the "sufficiency of accuracy" depended on project aims.<sup>46,47</sup> This involved using the model with calibrated parameters and comparing the model outputs to the observed

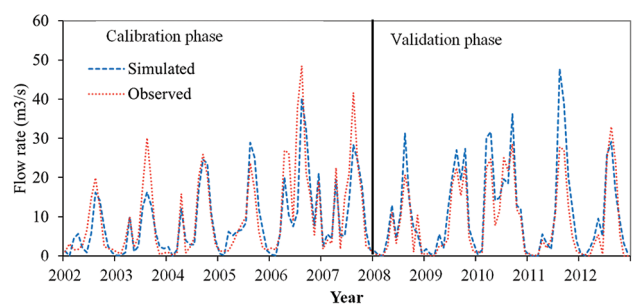


**Figure 4. Comparison of measured and simulated river flow during the calibration and validation phases**

**Table 3. Sensitivity analysis results**

Sensitivity rank	Parameters	Description	Parameter range	Fitted value
1	Curve number 2	Soil Conservation Service runoff curve number: Represents runoff potential based on land use, soil type, and cover.	±0.25	0.05
2	GW-DELAY	Groundwater delay: Time delay (in days) for groundwater flow to reach the stream channel, affecting baseflow dynamics.	0–500	59.4
3	CH-K2	Effective hydraulic conductivity in main channels: Influences baseflow and subsurface runoff through stream channels.	0–500	99.43
4	SOL-AWC	Available water capacity of soil layer: The soil’s capacity to store water; important for hydrological modeling.	±0.25	0.04
5	CANMAX	Maximum canopy storage: The amount of water the canopy can hold before it is lost to evaporation or throughfall.	0–100	0.48
6	ALPHA-BF	Baseflow alpha factor: Defines the rate of baseflow contribution to streamflow.	0–1	0.03
7	ESCO	Soil evaporation compensation factor: Adjusts soil evaporation based on moisture availability.	0–1	0.97
8	EPCO	Plant uptake compensation factor: Adjusts plant transpiration based on soil moisture availability.	0–1	0.96
9	GW-QMN	Threshold depth of water in the shallow aquifer: Depth at which groundwater starts contributing to baseflow.	0–500	179.75
10	SOL-K	Saturated hydraulic conductivity: The rate at which water can flow through saturated soil, affecting groundwater recharge.	±0.25	0.07
11	CH-N2	Manning’s value for main channels: Roughness coefficient for stream channels, influencing flow velocity and runoff.	0.01–0.3	0.14
12	SOL-Z	Depth from soil surface to bottom of layer: Specifies the depth of the soil profile, influencing water retention and plant root penetration.	±0.25	–0.02
13	RCHRG-DP	Deep aquifer percolation fraction: Fraction of water percolating into deep aquifers, influencing groundwater recharge.	0–1	0.24

data.<sup>37,38</sup> The analysis employed two primary measures for evaluating the SWAT model: NSE and  $R^2$ . These were the measures of a model’s accuracy, reproducibility, and ability to fit observed data.  $R^2$  represents the percentage of variance explained by the model and serves as a measure of goodness of fit, with values ranging from 0 to 1. It is computed as (Equation V):

$$R^2 = \frac{[\sum_i^n (Q_{obs} - Q_{mo})(Q_s - Q_{ms})]^2}{\sum_i^n (Q_{obs} - Q_{mo})^2 \sum_i^n (Q_s - Q_{ms})^2} \quad (V)$$

where  $Q_{obs}$  is the observed flow ( $m^3/s$ ) and  $Q_{mo}$  is its mean;  $Q_s$  is the simulated flow ( $m^3/s$ ) and  $Q_{ms}$  is its mean. An  $R^2$  of 1 indicates a perfect fit, while 0 suggests a poor accuracy. The NSE measures the residual error relative to the variance of the observed data.<sup>38,48</sup> The NSE value ranges from  $-\infty$  to 1, with values closer to 1 indicating a better fit between observed and simulated data. An NSE value  $>0$  suggests an acceptable model performance,

while values below 0 indicate poor model fit, meaning the simulated data does not closely match the observed flow values.<sup>37</sup> The calibration and validation results demonstrate that the SWAT model effectively simulates monthly river discharge in the region, with high  $R^2$  and NSE values indicating an accurate representation of hydrological dynamics (Table 4). The result aligns with the scholars’ recommendations.<sup>38</sup> In addition, the results are consistent with previous studies that demonstrated SWAT’s capability to model hydrological processes across various watersheds.<sup>49</sup> The model’s performance validated its reliability for predicting the future impacts of land-use changes on water resources, providing a robust tool for sustainable water resource planning and management. Table 4 presents the performance metrics for the SWAT model, including the calibration and validation results.

In Table 4,  $R^2$ , NSE, and PBIAS values highlight the model accuracy and reliability during calibration

**Table 4. The soil and water assessment tool model performance metrics**

Gauging station	Model stage	Objective function		
		R <sup>2</sup>	NSE	PBIAS
Germam	Calibration	0.84	0.75	-0.1
	Validation	0.79	0.72	-11

Abbreviations: NSE: Nash-sutcliffe efficiency; PBIAS: Percent bias.

and validation phases. The SWAT model performed well during both the calibration and validation periods. The model closely matched the observed data with an  $R^2$  of 0.84 during calibration and 0.79 in validation. The SWAT model accurately estimated groundwater recharge, with NSE values of 0.75 (calibration) and 0.72 (validation) and minimal bias (PBIAS: -0.1 and -11, respectively). These results confirm its reliability for water resource management in the region.

#### 2.2.8. Groundwater recharge estimation using the SWAT and change detection

In this study, groundwater recharge in the Dire Dawa watershed was assessed using the SWAT model, combined with remote sensing data and environmental variables. To isolate the impact of LULC changes on hydrological processes, change detection was performed using satellite imagery from 2000, 2010, and 2020. The LULC maps were compared using several methods, including image differencing, which highlighted significant land cover changes by subtracting one map from another; post-classified comparison, where each year's LULC map was independently classified and then compared to quantify the changes; and change matrix analysis, which assessed the accuracy of the LULC classifications and the nature of the transitions. These change detection results were integrated into the SWAT model to simulate how varying LULC scenarios influenced groundwater recharge and surface runoff. This approach provides a clear understanding of how LULC changes influence hydrological processes, while accounting for other factors that may affect groundwater recharge and surface runoff.

### 3. Results

#### 3.1. Accuracy assessment

This research utilized LULC maps from 2000, 2010, and 2022, created using ERDAS IMAGINE 2015 and ArcGIS 10.8 software. Ground truth data were collected using GPS and Google Earth Pro, achieving an accuracy

standard of 85% and a kappa coefficient of  $>0.85$ . In this study, 50 ground truth data points per land-use class in the watershed were utilized to optimize the accuracy of classification (Table 5). The accuracy assessment result achieved PA and UA values that met the required standard, allowing for further analysis.<sup>35</sup>

#### 3.2. LULC change

This study analyzed the effects of LULC changes on groundwater recharge in the Dire Dawa watershed from 2000 to 2022. Six dominant LULC classes, that is, shrubland, forest, agriculture, settlement, desert, and river sand, were identified for the years 2000, 2010, and 2022 (Figure 5). The results show that agricultural and built-up areas increased while shrubland decreased. In addition, forest land, which covered approximately 85.3 km<sup>2</sup> (12.1%) in 2000, was drastically reduced to 55.7 km<sup>2</sup> (7.9%) by 2010 (Table 6). These alterations are primarily attributed to agricultural expansion and urbanization in this region. Impunity led to changes in the watershed's hydrology, modifying water infiltration, soil erosion, evapotranspiration, and runoff patterns. These results highlight the growing problem of land degradation and underscore the importance of sustainable land management and soil conservation as a safeguard against groundwater depletion and maintaining hydrological equilibrium within the watershed.

Remotely sensed imagery plays a significant role in monitoring LULC conversion, offering high spatial and temporal resolution for area conversion. In this study, a mixed approach involving both supervised and unsupervised image classification was employed, as it is widely used in remote sensing data analysis. This method focuses on the transitions between LULC classes and provides explicit information, facilitating the interpretation of valuable patterns. Areal extent measurements across different temporal periods were used to estimate the magnitude of LULC changes. The results of the LULC change analysis for the years 2000, 2010, and 2022, presented in Figure 5 and Table 6, illustrate the spatial and temporal variability of LULC across the watershed during the study period.

#### 3.3. Hydrological impacts of LULC changes

The impacts of LULC changes on the groundwater recharge and surface runoff in the Dire Dawa watershed from 2000 to 2022 were evaluated using the SWAT model. The water balance components, specifically recharge and runoff, were estimated independently for each study period. Change detection was then conducted

**Table 5. Accuracy assessment result of LULC classification**

LULC classes	Shrubland	Agriculture	Forest	Built up	Bare land	Riverside sand	Total	Diagonal	UA (%)	PA (%)
Shrubland	10	0	0	0	0	0	10	10	100	77
Agriculture	1	7	0	0	0	0	8	7	88	78
Forest	1	0	7	0	0	0	8	7	88	100
Built up	0	1	0	7	0	0	8	7	88	100
Bare land	0	0	0	0	6	0	6	6	100	86
Riverside sand	1	1	0	0	1	7	10	7	70	100
Total	13	9	7	7	7	7	50	Overall accuracy (88%)		

Abbreviations: LULC: Land use and land cover; PA: Producer’s accuracy; UA: User accuracy.

**Table 6. Areal extent and relative change in land use and land cover (LULC) types**

LULC classes	Areal extent of LULC types						Relative change in LULC types					
	2000		2010		2022		2010–2000		2022–2010		2022–2000	
	km <sup>2</sup>	%	km <sup>2</sup>	%	km <sup>2</sup>	%	km <sup>2</sup>	%	km <sup>2</sup>	%	km <sup>2</sup>	%
Shrubland	352.4	49.9	322.2	45.6	269	38.1	-30.2	-8.6	-53.2	-16.5	-83.4	-23.7
Agricultural land	217.8	30.9	262	37.1	332.5	47.1	44.2	20.3	70.5	26.9	114.7	52.6
Forested land	85.3	12.1	55.7	7.9	31.7	4.5	-29.6	-34.7	-24	-43.1	-53.6	-62.8
Built-up area	22.6	3.2	35.5	5	40.5	5.7	12.9	57.1	5	14.1	17.9	79.2
Bare land	20	2.8	22	3.1	23.4	3.3	2	10	1.4	6.4	3.4	17
Riverside sand	7.7	1.1	8.6	1.2	8.8	1.2	0.9	11.7	0.2	2.3	1.1	14.3

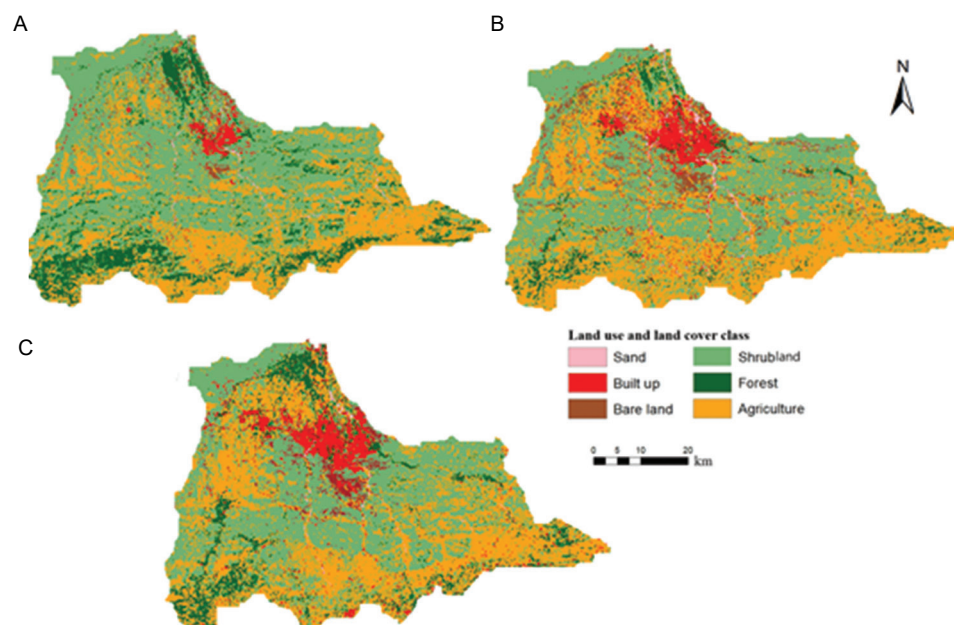


**Figure 5. Land use and land cover maps of the study area for (A) 2000, (B) 2010, and (C) 2022**

using GIS tools. To identify the impacts of LULC changes on groundwater recharge, all input factors used in the model, except the variable LULC, were kept constant. The analysis indicated that between 2000 and

2010, groundwater recharge decreased by 40.6 mm/y (20.4%), while surface runoff increased by 32.9 mm/y (15.3%). From 2010 to 2020, groundwater recharge continued to decline at a slower rate of 8.2 mm/y (5.2%),

while runoff rose by an additional 9.84 mm/y (4.0%). Over the entire study period, groundwater recharge decreased by 48.8 mm/y (24.5%), and surface runoff increased by 42.8 mm/y (19.9%). Table 7 presents the results of the change analysis.

These findings underscore the increasing pressure on water resources in the Dire Dawa watershed, resulting from urbanization and agricultural expansion. The SWAT model demonstrates how changes in land cover, such as the loss of shrubland and forests, disrupt the natural water cycle, leading to reduced groundwater recharge and increased surface runoff. To mitigate these effects, sustainable land management strategies, including ecosystem restoration and improved urban planning, are crucial for restoring the water balance in the region.

The areal variation of groundwater recharge over the Dire Dawa watershed is significant, with the highest recharge occurring in the eastern and northwestern sub-watersheds. In contrast, the central and northern regions have experienced a rapid decline in recharge (Figure 6). These results underscore the need for continuous, high-resolution monitoring to understand spatial and temporal effects of land-use changes on watershed hydrology. Maintaining a balance between land use and water resources is critical for the long-term sustainability of the watershed. Through adaptive management strategies, the sustainability of groundwater resources can be ensured, and the ecological integrity of the area, as well as the way of life that relies on its water supply, can be maintained.

#### 4. Discussion

Using the SWAT model, this study examined the impacts

**Table 7. Average annual recharge and surface runoff changes due to land use and land cover changes (2022–2000)**

Year	Simulated values			
	Groundwater recharge		Surface runoff	
	mm/y	%	mm/y	%
2000	199.4	39.2	215.2	29.8
2010	158.9	31.2	248.1	34.4
2022	150.7	29.6	258.0	35.8
Changes				
2010–2000	–40.6	–20.4	32.9	15.3
2022–2010	–8.2	–5.2	9.8	4.0
2022–2000	–48.8	–24.5	42.8	19.9

of LULC changes on groundwater recharge in the Dire Dawa watershed, Ethiopia, from 2000 to 2022. The analysis indicates significant transformations in LULC, where agricultural land expanded by 114.7 km<sup>2</sup> (52.6%), built-up areas increased by 17.8 km<sup>2</sup> (79.2%), shrublands decreased by 83.4 km<sup>2</sup> (23.7%), and the forested regions declined by 53.6 km<sup>2</sup> (62.8%). The hydrological modeling results demonstrate that these LULC changes substantially reduced groundwater recharge by 48.8 mm/y (24.5%) and increased surface runoff by 42.8 mm/y (19.9%). These findings underscore the urgent need for sustainable land and water management strategies in the region. The SWAT model performance was assessed using key statistical metrics:  $R^2$  values of 0.84 and 0.79, NSE values of 0.75 and 0.72, and PBIAS values of –0.1 and –11 during the calibration and validation periods, respectively. Based on established evaluation benchmarks, these results indicate strong model performance, characterized by high  $R^2$  and NSE values and low PBIAS.<sup>47</sup> The model effectively simulates the hydrological processes within the study area and is well-suited for projecting river discharge and assessing future hydrological changes driven by land-use changes and climate variations.

The study by Jin *et al.*,<sup>50</sup> in the Jing River basin in China, demonstrated that LULC changes significantly reduced runoff and altered hydrological cycle processes. These findings align with those of the present study, confirming that urbanization and deforestation contribute to increased surface runoff and reduced groundwater recharge. Similarly, Lindle *et al.*<sup>51</sup> investigated groundwater recharge in the Limpopo province, South Africa, and revealed that ephemeral river flow and LULC changes significantly influence recharge rates. This supports the conclusion that land-use changes disrupt natural recharge mechanisms, highlighting the need for improved water resource management. In another related study, Mechal *et al.*<sup>13</sup> analyzed groundwater recharge in the Ziway Lake watershed of the Ethiopian Rift using the SWAT model and concluded that recharge rates vary significantly due to topographic and climatic influences. This finding is comparable to the present study's results, which show that climate variability and terrain characteristics play pivotal roles in recharge patterns. Collectively, these studies reinforce the importance of integrating climate variability into land-use planning.

The study by Bucha *et al.*<sup>25</sup> in Ethiopia's Lake Chamo sub-basin observed increased surface runoff and decreased infiltration due to land-use changes, aligning with the present study's conclusions. Additional studies support these findings. For example, a study of the

## SWAT-based LULC impacts on groundwater recharge

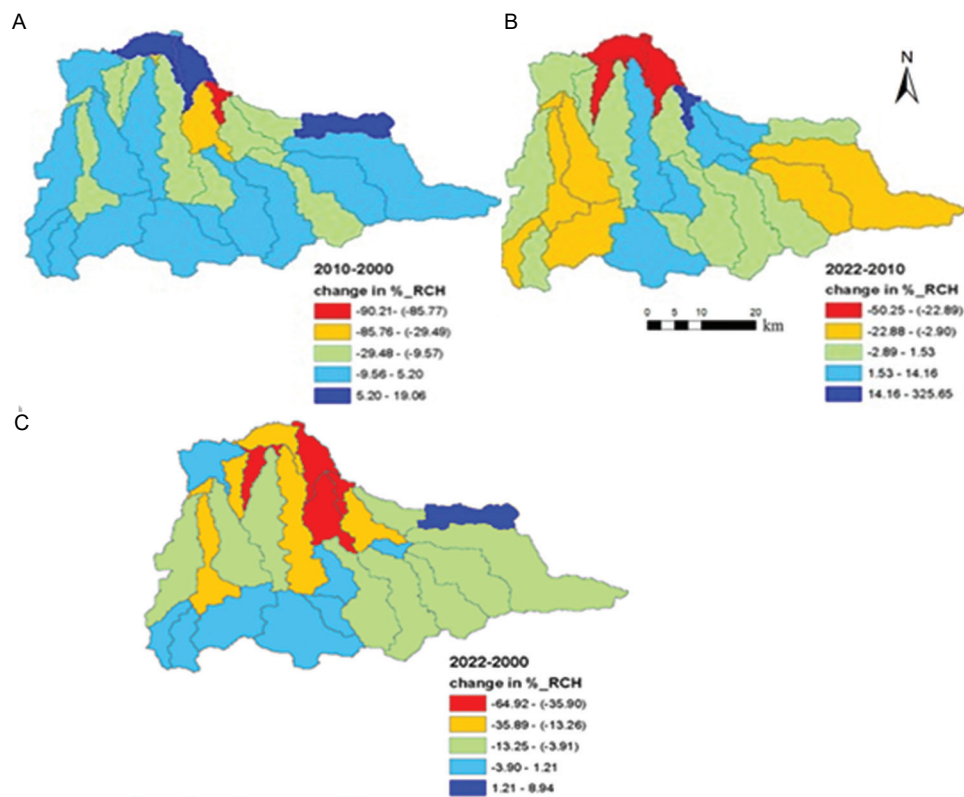


**Figure 6. Groundwater recharge (RCH) changes due to land use and land cover: (A) 2010–2000, (B) 2022–2010, and (C) 2022–2000**

Kanari River in India used the SWAT model to estimate groundwater recharge and surface runoff, revealing that 46.2% of precipitation contributed to surface runoff.<sup>20</sup> With NSE values of 0.83 and 0.71 for the calibration and validation, respectively, the model demonstrated good performance in hydrological assessment. Likewise, Yifru *et al.*<sup>18</sup> in South Korea integrated SWAT-MODFLOW to analyze spatiotemporal variations in groundwater recharge, demonstrating improved low-streamflow estimations and highlighting the benefits of coupling hydrological models. In the Afram Plains watershed of Ghana, a GIS-based recharge zone mapping approach categorized recharge potential into various zones, emphasizing the importance of spatial analysis in groundwater assessment.<sup>52</sup> The Olifants basin study in Southern Africa reported significant declines in groundwater recharge due to urbanization and agricultural expansion,<sup>14</sup> mirroring the present study's findings on LULC impacts. Meanwhile, the Lower Chenab Canal irrigation study in the Indus Basin projected a 37–40% increase in groundwater recharge under climate change scenarios,<sup>53</sup> contrasting with the declining recharge trends in the Dire Dawa watershed, highlighting the significance of regional climatic

variability on groundwater dynamics.

This study utilized the SWAT model, which, despite its widespread application, carries inherent uncertainties related to land-use classifications. The accuracy of LULC change detection was influenced by the classification techniques used; although ERDAS IMAGINE and GIS tools were employed, potential errors in classification could have impacted the results. Future research should integrate climate models to assess the combined impacts of LULC changes and climate change on hydrological processes. Incorporating remote sensing techniques and machine learning approaches could enhance prediction accuracy. Furthermore, policy-oriented studies examining the socio-economic drivers of LULC change and their implications for sustainable water resource management would be valuable.

## 5. Conclusion

This study examined how LULC changes affect groundwater recharge and surface runoff in the Dire Dawa watershed from 2000 to 2022. Using remote sensing and GIS data, alongside the SWAT hydrological model, the research provides compelling evidence

of how human-driven landscape transformations are impacting the region's water resources. The SWAT model, calibrated and validated using the SUFI-2 method, showed strong performance, with  $R^2$  values of 0.84 and 0.79, NSE values of 0.75 and 0.72, and PBIAS values of  $-0.1$  and  $-11$  for calibration and validation, respectively. Over the past two decades, forests and shrublands in the watershed have steadily declined, replaced by expanding agricultural lands and urban areas. These shifts have altered the watershed's hydrological behavior, reducing its capacity to absorb and store water. SWAT model results indicate a 24.5% decrease in groundwater recharge and a 19.9% increase in surface runoff during the study period. SWAT-CUP simulations further confirmed a 20% reduction in recharge, primarily linked to deforestation, urban growth, and agricultural expansion.

Land-use analysis showed a 79.2% increase in built-up areas and a 52.6% rise in agricultural land, while scrubland and forest areas decreased by 23.7% and 62.8%, respectively. These changes demonstrate the direct and measurable impact of LULC transformation on the watershed's hydrological system. The findings serve as a clear call to action: Without integrated and sustainable land management strategies, the Dire Dawa watershed will continue to face declining water availability and increased runoff risks. Protecting natural land cover, guiding urban expansion, and promoting sustainable agricultural practices are essential steps to preserving this vital ecosystem and its water resources for future generations.

To restore balance in the region's water cycle, this study recommends adopting sustainable land management practices. The findings offer important policy implications for protecting groundwater resources and ultimately achieving water security in a future characterized by expanding anthropogenic stress. Key recommendations include reforestation, improved agricultural methods, and efficient urban planning strategies to mitigate the adverse effects of rapid urbanization and land degradation. The effective management of groundwater recharge, through both conservation and sustainable development practices, will be a key to meeting future water needs and supporting regional resilience to climate change and population growth. This study contributes to the development of effective hydrological management strategies that address the immediate challenges of groundwater depletion in the study area and lay the foundation for sustainable watershed management in Ethiopia. Moreover, the findings offer insights that

could be applicable to other regions facing similar environmental pressures, thereby supporting the resilience of both human and ecological systems globally. Future research is encouraged to integrate the MODFLOW groundwater model with the SWAT hydrological model. Such integration could enhance the accuracy of groundwater recharge estimates by more effectively capturing surface water-groundwater interactions, thereby improving model reliability and informing more effective water resource management strategies.

### Acknowledgments

The authors would like to acknowledge the National Meteorological Institute and the Ministry of Water and Energy of Ethiopia for providing meteorological and hydrological data, respectively.

### Funding

None.

### Conflict of interest

The authors declare no conflicts of interest related to this work or with any institution or organization.

### Author contributions

*Conceptualization:* Tariku Takele, Adula Bayisa

*Data curation:* Tariku Takele, Adula Bayisa

*Methodology:* Tariku Takele, Adula Bayisa

*Supervision:* Tariku Takele, Muralitharan Jothimani

*Validation:* All authors

*Visualization:* All authors

*Writing—original draft:* Tariku Takele, Adula Bayisa

*Writing—review & editing:* All authors

### Availability of data

The data used in this study are available from the corresponding author on reasonable request.

### References

1. Krueger E, Rao PSC, Borchardt D. Quantifying urban water supply security under global change. *Glob Environ Change*. 2019;56:66-74. doi: 10.1016/j.gloenvcha.2019.03.00
2. Adger WN, Crépin AS, Folke C, *et al.* Urbanization,

- migration, and adaptation to climate change. *One Earth*. 2020;3(4):396-399.  
doi: 10.1016/j.oneear.2020.09.016
3. Takele T, Mechal A, Berhe BA. Evaluation of groundwater recharge potential using geospatial analysis in the Ziway Lake Watershed, Ethiopian Rift: A GIS and AHP-based methodological framework. *Environ Sustain Indic*. 2025;26:100692.  
doi: 10.1016/j.indic.2025.100692
  4. Ogbu KN, Ndulue EL, Ahaneku IE, Ubah IJ. Evaluation of the impact of climate change on streamflow using SWAT model. *ASM Sci J*. 2020;13:1-8.  
doi: 10.32802/asmscj.2020.494
  5. Das SK, Ahsan A, Khan M.H.R.B., Tariq M.A.U.R., Muttil, N., Ng, A.W.M. Impacts of climate alteration on the hydrology of the Yarra River Catchment, Australia using GCMs and SWAT model. *Water*. 2022;14(3):445.  
doi: 10.3390/w14030445
  6. Tola TL, Zhang K, Chukalla AD, *et al*. Spatiotemporal lakes surface area changes over 35 years and potential causes in the Central Rift Valley, Ethiopia. *J Hydrol Reg Stud*. 2024;54:101863.  
doi: 10.1016/j.ejrh.2024.101863
  7. Ware HH, Chang SW, Lee JE, Chung IM. Assessment of hydrological responses to land use and land cover changes in forest-dominated watershed using SWAT model. *Water*. 2024;16(4):528.  
doi: 10.3390/w16040528
  8. Zhao J, Zhang N, Liu Z, Zhang Q, Shang C. SWAT model applications: From hydrological processes to ecosystem services. *Sci Total Environ*. 2024;931:172605.  
doi: 10.1016/j.scitotenv.2024.172605
  9. Oo HT, Zin WW, Kyi CCT. Analysis of streamflow response to changing climate conditions using SWAT model. *Civil Eng J*. 2020;6(2):194-209.  
doi: 10.28991/cej-2020-03091464
  10. Mechal A, Birk S, Dietzel M, *et al*. Groundwater flow dynamics in the complex aquifer system of Gidabo River Basin (Ethiopian Rift): A multi-proxy approach. *Hydrogeol J*. 2016;25(2):519-538.  
doi: 10.1007/s10040-016-1489-5
  11. Hoogesteger J. Regulating agricultural groundwater use in arid and semi-arid regions of the Global South: Challenges and socio-environmental impacts. *Curr Opin Environ Sci Health*. 2022;27:100341.  
doi: 10.1016/j.coesh.2022.100341
  12. Hailesilassie W, Tegaye T. Comparative assessment of the water quality deterioration of Ethiopian Rift lakes: The case of Lakes Ziway and Hawassa. *Environ Earth Sci Res J*. 2019;6(4):162-166.  
doi: 10.18280/eesrj.060403
  13. Mechal A, Takele T, Meten M, Deyassa G, Degu Y. A modeling approach for evaluating the impacts of land use/land cover change for Ziway Lake Watershed hydrology in the Ethiopian Rift. *Model Earth Syst Environ*. 2022;8(4):4793-4813.  
doi:10.1007/s40808-022-01472-w
  14. Chen P, Ma X, Ma J, *et al*. Discrepancy and estimates of groundwater recharge under different land use types on the Loess Plateau. *J Hydrol Reg Stud*. 2024;53:101793.  
doi: 10.1016/j.ejrh.2024.101793
  15. Musie M, Sen S, Chaubey I. Hydrologic responses to climate variability and human activities in Lake Ziway Basin, Ethiopia. *Water*. 2020;12(1):164.  
doi: 10.3390/w12010164
  16. Zhang Z, Si H, Feng B, Wang Y, Lv M, Wagan B. Research of hydrological responses to land-use variability in a semiarid watershed based on SWAT model. *Fresenius Environ Bull*. 2014;23(5):1190-1197.
  17. Mosase E, Ahiablame L, Park S, Bailey R. Modelling potential groundwater recharge in the Limpopo River Basin with SWAT-MODFLOW. *Groundw Sustain Dev*. 2019;9:100260.  
doi: 10.1016/j.gsd.2019.100260
  18. Yifru BA, Chung IM, Kim MG, Chang SW. Assessment of groundwater recharge in agro-urban watersheds using integrated SWAT-MODFLOW model. *Sustainability*. 2020;12(16):6593.  
doi: 10.3390/su12166593
  19. Takele T, Mechal A, Berhe BA. Assessing groundwater potential in the Ziway Lake Watershed using geographical information system, analytic hierarchy process, and drinking water quality index. *Glob Chall*. 2025;9:2400354.  
doi: 10.1002/gch2.202400354
  20. Trivedi A, Awasthi MK, Nandeha N, Gautam VK, Mehla MK. Addressing water security challenges through groundwater recharge for revival of Kanari River using AHP and geospatial techniques. *Discover Water*. 2024;4(1):59.  
doi: 10.1007/s43832-024-00124-7
  21. Arnold JG, Srinivasan R, Muttiyah RS, Williams JR. Large area hydrologic modeling and assessment part I: model development. *J Am Water Resour Assoc*. 1998;34(1):73-89.  
doi: 10.1111/j.1752-1688.1998.tb05961.x
  22. Wagner PD, Bieger K, Arnold JG, Fohrer N. Representation of hydrological processes in a rural lowland catchment in Northern Germany using SWAT and SWAT+. *Hydrol Process*. 2022;36(5):e14589.  
doi: 10.1002/hyp.14589
  23. Sakulchai EKS, Charoen SY, Kamolsin YP. Assessment of the impact of land use change on runoff in Lam Phachi Basin using satellite data and SWAT model. *Kasetsart Univ J Sci Technol*. 2018;7(3):11-26.
  24. Desta H, Lemma B. SWAT based hydrological assessment and characterization of Lake Ziway sub-watersheds, Ethiopia. *J Hydrol Reg Stud*. 2017;13:122-137.  
doi: 10.1016/j.ejrh.2017.08.002
  25. Bucha NM, Goshime DW, Awas AA, Asnake AB.

- Hydrologic responses contemplating to land use land cover change and water balance of Lake Chamo sub-basin of Ethiopia. *Sustain Water Resour Manag.* 2024;10(1):29.  
doi: 10.1007/s40899-023-01003-0
26. Kenea U, Adeba D, Regasa M, Nones M. Hydrological responses to land use land cover changes in the Fincha'a Watershed, Ethiopia. *Land.* 2021;10(9):916.  
doi: 10.3390/land10090916
  27. Beker BA, Kansal ML. Complexities of the urban drinking water systems in Ethiopia and possible interventions for sustainability. *Environ Dev Sustain.* 2023;26(2):4629-4659.  
doi: 10.1007/s10668-022-02901-7
  28. Gonza DK, Tekleweld FA, Hishe TG, Shumey EE, Birhane BS. Performance analysis of water meters for measuring domestic water consumption, the case of Dire Dawa, Ethiopia. *Int J Energy Water Resources.* 2021;5:405-412.  
doi: 10.1007/s42108-021-00130-8
  29. Tenaw D, Assfaw A. Households willingness to pay for improved urban water supply in Dire Dawa city administration: The role of socio-economic factors and water supply-related perceptions. *Sustain Water Resour Manag.* 2022;8(1):24.  
doi: 10.1007/s40899-022-00625-0
  30. Erena SH, Worku H. Dynamics of land use land cover and resulting surface runoff management for environmental flood hazard mitigation: The case of Dire Dawa city, Ethiopia. *J Hydrol Reg Stud.* 2019;22:100598.  
doi: 10.1016/j.ejrh.2019.100598
  31. Tilahun K, Merkel BJ. Estimation of groundwater recharge using a GIS-based distributed water balance model in Dire Dawa, Ethiopia. *Hydrogeol J.* 2009;17(6):1443-1457.  
doi: 10.1007/s10040-009-0455-x
  32. Beyene AD, Shumetie A. *Green Legacy Initiative for Sustainable Economic Development in Ethiopia.* Addis Ababa. Ethiopia: Ethiopian Economic Association (EEA); 2023.
  33. Desta H, Fetene A. Land-use and land-cover change in Lake Ziway watershed of the Ethiopian Central Rift Valley Region and its environmental impacts. *Land Use Policy.* 2020;96:104682.  
doi: 10.1016/j.landusepol.2020.104682
  34. Teklay A, Dile YT, Asfaw DH, Bayabil HK, Sisay K. Impacts of climate and land use change on hydrological response in Gumara Watershed, Ethiopia. *Ecohydrol Hydrobiol.* 2020;21(2):315-332.  
doi: 10.1016/j.ecohyd.2020.12.001
  35. Foody GM, Mathur A. A relative evaluation of multiclass image classification by support vector machines. *IEEE Trans Geosci Remote Sens.* 2004;42(6):1335-1343.  
doi: 10.1109/tgrs.2004.827257
  36. Ougahi JH, Karim S, Mahmood SA. Application of the SWAT model to assess climate and land use/cover change impacts on water balance components of the Kabul River Basin, Afghanistan. *J Water Clim Change.* 2022;13(11):3977-3999.  
doi: 10.2166/wcc.2022.261
  37. Abbaspour KC. SWAT calibration and uncertainty programs: A user manual. 2015;103:17-66.
  38. Abbaspour KC, Vejdani M, Haghghat S. *MODSIM07 - Land, Water and Environmental Management: Integrated Systems for Sustainability, Proceedings;* 2007.
  39. Soil Conservation Service (SCS). *National Engineering Handbook, Section 4: Hydrology.* Department of Agriculture, Washington DC; 1972. p.762.
  40. Hargreaves GH, Samani ZA. Estimating potential evapotranspiration. *J Irrig Drain Div.* 1982;108(3):225-230.  
doi: 10.1061/jrcea4.0001390
  41. Arnold JG, Kiniry JR, Srinivasan R, Williams JR, Haney EB, Neitsch SL. *Soil and Water Assessment Tool: Input/Output Documentation.* Version 2012. TR-439. United States: Texas Water Resources Institute, College Station; 2012. p. 1-650.
  42. Fuka DR, Walter MT, MacAlister C, Steenhuis TS, Easton ZM. SWATModel: A multi-operating system, multi-platform SWAT model package in R. *J Am Water Resour Assoc.* 2014;50(5):1349-1353.  
doi: 10.1111/jawr.12170
  43. Arnold J, Srinivasan R, Neitsch S, et al. *Soil and Water Assessment Tool (SWAT) Global Applications.* Bangkok, Thailand: World Association of Soil and Water Conservation; 2009.
  44. Neitsch SL, Williams JR, Arnold JG, Kiniry JR. *Soil and Water Assessment Tool Theoretical Documentation.* Version 2009. United States: Texas Water Resources Institute, College Station; 2011.
  45. Bailey RT, Park S, Bieger K, Arnold JG, Allen PM. Enhancing SWAT+ simulation of groundwater flow and groundwater-surface water interactions using MODFLOW routines. *Environ Model Softw.* 2020;126:104660.  
doi: 10.1016/j.envsoft.2020.104660
  46. Pandit A, Hogan S, Mahoney DT, et al. Establishing performance criteria for evaluating watershed-scale sediment and nutrient models at fine temporal scales. *Water Res.* 2025;274:123156.  
doi: 10.1016/j.watres.2025.123156
  47. Moriasi DN, Gitau MW, Daggupati P, Pai N. Hydrologic and water quality models: Performance measures and evaluation criteria. *Trans ASABE.* 2015;58(6):1763-1785.  
doi: 10.13031/trans.58.10715
  48. Mengistu AG, Van Rensburg LD, Woyessa YE. Techniques for calibration and validation of SWAT model in data scarce arid and semi-arid catchments in South Africa. *J Hydrol Reg Stud.* 2019;25:100621.  
doi: 10.1016/j.ejrh.2019.100621

SWAT-based LULC impacts on groundwater recharge

49. Mechal A, Wagner T, Birk S. Recharge variability and sensitivity to climate: The example of Gidabo River Basin, Main Ethiopian Rift. *J Hydrol Reg Stud.* 2015;4:644-660.  
doi: 10.1016/j.ejrh.2015.09.001
50. Jin T, Zhang X, Xie J, Liang J, Wang T. Study on hydrological response of runoff to land use change in the Jing River Basin, China. *Environ Sci Pollut Res.* 2023;30(45):101075-101090.  
doi: 10.1007/s11356-023-29526-1
51. Lindle J, Villholth KG, Ebrahim GY, Sorensen JPR, Taylor RG, Jensen KH. Groundwater recharge influenced by ephemeral river flow and land use in the semiarid Limpopo Province of South Africa. *Hydrogeol J.* 2023;31(8):2291-2306.  
doi: 10.1007/s10040-023-02682-x
52. Dekongmen BW, Anornu GK, Kabo-Bah AT, et al. Groundwater recharge estimation and potential recharge mapping in the Afram Plains of Ghana using SWAT and remote sensing techniques. *Groundwater Sustain Dev.* 2022;17:100741.  
doi: 10.1016/j.gsd.2022.100741
53. Awan UK, Ismaeel A. A new technique to map groundwater recharge in irrigated areas using a SWAT model under changing climate. *J Hydrol.* 2014;519:1368-1382.  
doi: 10.1016/j.jhydrol.2014.08.049